LETTER

doi:10.1038/nature25172

Precision editing of the gut microbiota ameliorates colitis

Wenhan Zhu[1]*, Maria G. Winter[1]*, Mariana X. Byndloss[2], Luisella Spiga[1], Breck A. Duerkop[3], Elizabeth R. Hughes[1], Lisa Büttner[1], Everton de Lima Romão[2], Cassie L. Behrendt[3], Christopher A. Lopez[2], Luis Sifuentes-Dominguez[4], Kayci Huff-Hardy[5], R. Paul Wilson[6]†, Caroline C. Gillis[1], Çagla Tükel[6], Andrew Y. Koh[1,4], Ezra Burstein[5], Lora V. Hooper[3,7], Andreas J. Bäumler[2] & Sebastian E. Winter[1]

Inflammatory diseases of the gastrointestinal tract are frequently associated with dysbiosis[1–8], characterized by changes in gut microbial communities that include an expansion of facultative anaerobic bacteria of the Enterobacteriaceae family (phylum Proteobacteria). Here we show that a dysbiotic expansion of Enterobacteriaceae during gut inflammation could be prevented by tungstate treatment, which selectively inhibited molybdenum-cofactor-dependent microbial respiratory pathways that are operational only during episodes of inflammation. By contrast, we found that tungstate treatment caused minimal changes in the microbiota composition under homeostatic conditions. Notably, tungstate-mediated microbiota editing reduced the severity of intestinal inflammation in mouse models of colitis. We conclude that precision editing of the microbiota composition by tungstate treatment ameliorates the adverse effects of dysbiosis in the inflamed gut.

In genetically susceptible rodents, a dysbiotic microbiota is vertically transmissible; the affected offspring are more likely to develop intestinal inflammation[3,9,10], suggesting that components of the microbiota can instigate host responses in a disease-prone setting. The close association between mucosal inflammation and gut-microbiota dysbiosis poses a challenge to establishing causality between these two events. Using metagenomic sequencing, we recently identified molybdenum-cofactor-dependent metabolic pathways as a signature of inflammation-associated dysbiosis[11]. Molybdenum-cofactor-dependent anaerobic respiratory enzymes and formate dehydrogenases contribute independently to the bloom of model Enterobacteriaceae such as *Escherichia coli*[11,12]. We reasoned that identification of molybdenum-cofactor-dependent processes as drivers of dysbiosis would allow us to devise a strategy to manipulate microbiota metabolism and composition during gut inflammation. Selective editing of the microbiota would enable investigation of potential consequences of dysbiosis, such as exacerbation of mucosal inflammation.

Tungsten (W) can replace molybdenum in the molybdopterin cofactor, rendering this cofactor inactive in Enterobacteriaceae[13]. Supplementation of growth media with sodium tungstate does not have a general effect on growth of Enterobacteriaceae under standard aerobic laboratory conditions, but it abolishes anaerobic nitrate-reductase activity[13] in commensal *E. coli*, *Proteus* spp., and *Enterobacter cloacae* (Fig. 1a–c, Extended Data Fig. 1a). To test whether tungstate supplementation could negate the fitness advantage conferred by anaerobic respiration and formate oxidation *in vitro*, we analysed anaerobic growth of wild-type *E. coli* strains (K-12 and Nissle 1917) and isogenic molybdenum-cofactor biosynthesis-deficient mutants (Δ*moaA*) in mucin broth supplemented with sodium tungstate (Fig. 1d, e, Extended Data Fig. 1b). In the presence of an electron acceptor such as nitrate, or an electron donor such as formate, the wild-type strains outcompeted the isogenic *moaA* mutants, but this fitness advantage was abrogated by the addition of tungstate (Fig. 1d, e, Extended Data Fig. 1b).

To investigate whether tungstate could inhibit molybdenum-cofactor-dependent processes in the mammalian gut, we used a mouse model of chemically induced colitis (dextran sulfate sodium (DSS)-induced colitis) in conjunction with experimentally introduced *E. coli* indicator strains. Groups of DSS- and mock-treated C57BL/6 mice were inoculated orally with an equal mixture of the *E. coli* K-12 wild-type strain and the Δ*moaA* mutant after the onset of inflammation. Colonization of the caecum and colon lumen was assessed five days after inoculation (Fig. 1f, g, Extended Data Fig. 2a). Prior to inoculation with *E. coli* K-12, we were unable to isolate any endogenous Enterobacteriaceae family members from these animals. Consistent with previous results[12], the K-12 wild-type strain outcompeted the Δ*moaA* mutant in the caecal and colonic content of DSS-treated mice (Fig. 1f). Administration of tungstate in the DSS-induced-colitis model abrogated the fitness advantage conferred by molybdenum-cofactor-dependent enzymes (Fig. 1f) and decreased overall numbers of *E. coli* K-12 in the gut lumen by several orders of magnitude (Fig. 1g). Similar observations were made using the human *E. coli* strain Nissle 1917 (Fig. 1h, Extended Data Fig. 3a, b) and a mouse *E. cloacae* strain (Fig. 1i, Extended Data Fig. 4a, b). Furthermore, the adherent-invasive *E. coli* (AIEC) strain NRG857c, originally isolated from a patient with inflammatory bowel disease, outcompeted the isogenic Δ*moaA* mutant in the intestinal content of DSS-treated mice (Fig. 1j). Tungstate administration negated the fitness advantage conferred by molybdenum-cofactor biosynthesis and reduced NRG857c colonization (Fig. 1j, Extended Data Figs 1c, 4c). Similarly, tungstate treatment decreased intestinal colonization by the mouse AIEC strain NC101 in a piroxicam-accelerated *Il10*$^{-/-}$ mouse model of colitis (Fig. 1k). Taken together, these experiments based on bacterial model organisms indicate that orally administered tungstate inhibits the molybdenum-cofactor-dependent bloom of Enterobacteriaceae in mouse models of colitis.

Next, we investigated the effect of tungstate treatment on the microbiota. C57BL/6 mice that naturally harboured endogenous Enterobacteriaceae were treated with DSS, DSS plus tungstate, tungstate alone or mock treatment. After nine days, DNA extracted from the caecal content was analysed by shotgun-metagenomic sequencing and 16S profiling (Fig. 2, Extended Data Fig. 2b). Intestinal inflammation was accompanied by changes in the predicted coding capacity of

[1]Department of Microbiology, University of Texas Southwestern Medical Center, 5323 Harry Hines Boulevard, Dallas, Texas 75390, USA. [2]Department of Medical Microbiology and Immunology, School of Medicine, University of California, Davis, One Shields Avenue, Davis, California 95616, USA. [3]Department of Immunology, University of Texas Southwestern Medical Center, 5323 Harry Hines Boulevard, Dallas, Texas 75390, USA. [4]Department of Pediatrics, University of Texas Southwestern Medical Center, 5323 Harry Hines Boulevard, Dallas, Texas 75390, USA. [5]Department of Internal Medicine, Division of Digestive & Liver Diseases, University of Texas Southwestern Medical Center 75390, 5323 Harry Hines Boulevard, Dallas, Texas, USA. [6]Department of Microbiology and Immunology, Lewis Katz School of Medicine, Temple University, 1801 North Broad Street, Philadelphia, Pennsylvania 19122, USA. [7]Howard Hughes Medical Institute, University of Texas Southwestern Medical Center, 5323 Harry Hines Boulevard, Dallas, Texas 75390, USA. †Present address: GlaxoSmithKline, 1250 South Collegeville Road, Collegeville, Pennsylvania 19426, USA. *These authors contributed equally to this work.

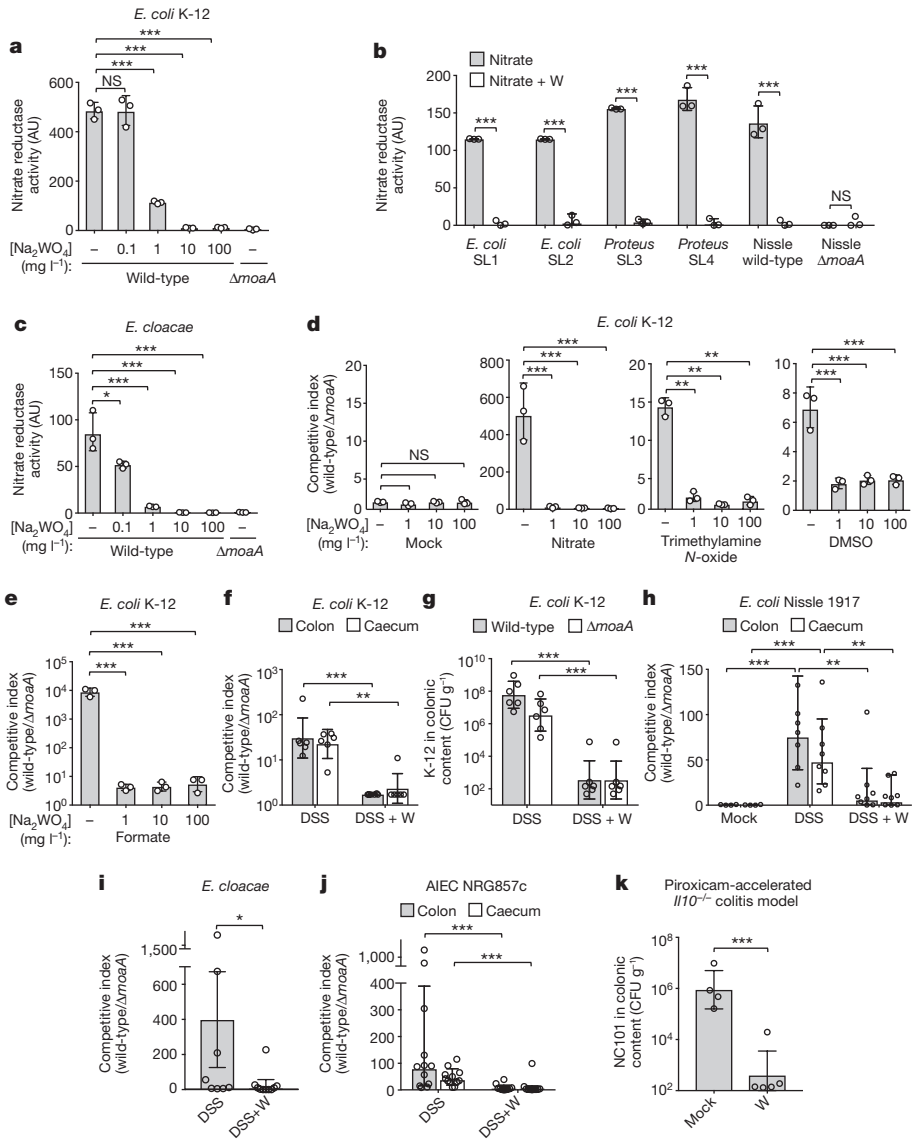

Figure 1 | Effect of tungstate on molybdenum cofactor-dependent anaerobic respiration. **a**–**c** Nitrate reductase activity in *E. coli* K-12 (**a**), isolated commensal Enterobacteriaceae strains SL1–SL4 and *E. coli* Nissle 1917 (**b**; strains are described in Supplementary Table 1), and an *Enterobacter cloacae* strain (**c**). W, tungstate (Na_2WO_4); AU, arbitrary units. **d**, **e**, Competitive anaerobic growth of the *E. coli* K-12 wild type and a *moaA* mutant (Δ*moaA*) in the presence of electron acceptors (**d**) or microaerobic growth with the electron donor formate (**e**). In **a**–**e**, $n = 3$ biological replicates for each condition. **f**–**j**, C57BL/6 mice received tungstate, DSS, or both (DSS+W) in drinking water for four days. Animals were inoculated intragastrically with an equal mixture of the indicated *E. coli* wild-type strains and isogenic *moaA* mutants. *E. coli* populations in the caecal and colonic content were analysed five days after inoculation: competitive index (**f**) and total population (**g**) of *E. coli* K-12; competitive index for Nissle 1917 (**h**), *E. cloacae* (**i**) and NRG857c (**j**). CFU, colony-forming units. In **f**, **g**: $n = 6$ per group. In **h**: Mock, $n = 4$; DSS, $n = 8$; DSS+W, $n = 8$. In **i**: DSS, $n = 8$; DSS+W, $n = 10$. In **j**: DSS, $n = 12$; DSS+W, $n = 10$. **k**, *Il10*$^{-/-}$ mice on piroxicam-fortified diet were inoculated intragastrically with the mouse strain NC101 and received tungstate in drinking water or mock treatment. The abundance of *E. coli* NC101 was assessed after 14 days (mock, $n = 4$; W, $n = 5$). Unless stated otherwise, n indicates the number of animals per group. Data are shown as geometric mean and geometric s.d.; $^*P < 0.05$; $^{**}P < 0.01$; $^{***}P < 0.001$; NS, not statistically significant.

the microbiota (Fig. 2a). As found in a recent metagenomic analysis of mock and DSS-treated animals[11], molybdenum-cofactor-dependent processes such as nitrate respiration, trimethylamine *N*-oxide respiration and formate oxidation were overrepresented[11] (Fig. 2b, Extended Data Fig. 5a). Tungstate administration during colitis abolished these alterations in the metagenome (Fig. 2b, Extended Data Fig. 5a). Mirroring these changes in coding capacity, tungstate treatment during DSS-induced colitis shifted the microbial community profile from a dysbiotic state towards the normal state (Fig. 2c–e, Extended Data Fig. 5b). Consistent with the idea that molybdenum-cofactor-dependent processes contribute to the inflammation-associated bloom of *E. coli* and other Enterobacteriaceae, tungstate administration selectively blunted the expansion of the Enterobacteriaceae population, whereas other major taxonomic families were only marginally affected (Fig. 2e–g, Extended Data Fig. 5c).

In the absence of inflammation, tungstate treatment did not affect the coding capacity, diversity, community structure, or population of native Enterobacteriaceae (Fig. 2c, e, f, Extended Data Figs 5b, c, 6a). Obligate anaerobic commensals such as *Bacteroides* spp. perform a rudimentary form of anaerobic respiration by reducing endogenous fumarate to succinate. The *Bacteroides* fumarate reductase is not predicted to contain a molybdenum-cofactor-binding site and tungstate treatment had no significant effect on the prevalence of predicted fumarate-reduction pathways in the microbiome (Extended Data Fig. 6b). Furthermore, *in vivo* tungstate treatment did not affect butyrate production pathways, a major metabolic function of the microbiota (Extended Data Fig. 6c). Supplementation of growth media with tungstate did not inhibit bacterial growth or production of succinate and butyrate by *Bacteroides* and *Clostridium* strains *in vitro* (Extended Data Fig. 6d–h). We did not observe any negative effects of tungstate on the mouse host (Extended Data Fig. 7). Collectively, these experiments support the idea that tungstate inhibits the inflammation-associated changes in gut microbiota composition that are driven by molybdenum-cofactor-dependent metabolic pathways, in particular the inflammation-associated expansion of the Enterobacteriaceae population.

We then explored the consequences of tungsten-mediated microbiota editing on mucosal inflammation in the DSS-induced-colitis model. We analysed pathological changes, colon length, mRNA levels of pro-inflammatory markers in the caecum and proximal colon, and animal body weight in mice harbouring endogenous Enterobacteriaceae in the DSS-induced-colitis model. We also analysed mice that were experimentally colonized with *E. coli* strains K-12, Nissle 1917, AIEC NRG857c or *E. cloacae*. Administration of tungstate significantly reduced inflammatory markers and pathological changes in the large intestinal mucosa, rescued the inflammation-associated reduction of colon length and ameliorated body weight loss (Fig. 3a–c, Extended Data Figs 2c–l, 3c–h, 4d–h). This was not due to reduced DSS intake during treatment (Extended Data Fig. 8a). Similarly, tungstate administration in a piroxicam-accelerated *Il10*$^{-/-}$ colitis model reduced intestinal inflammation (Fig. 3d–g). These findings raised the possibility that

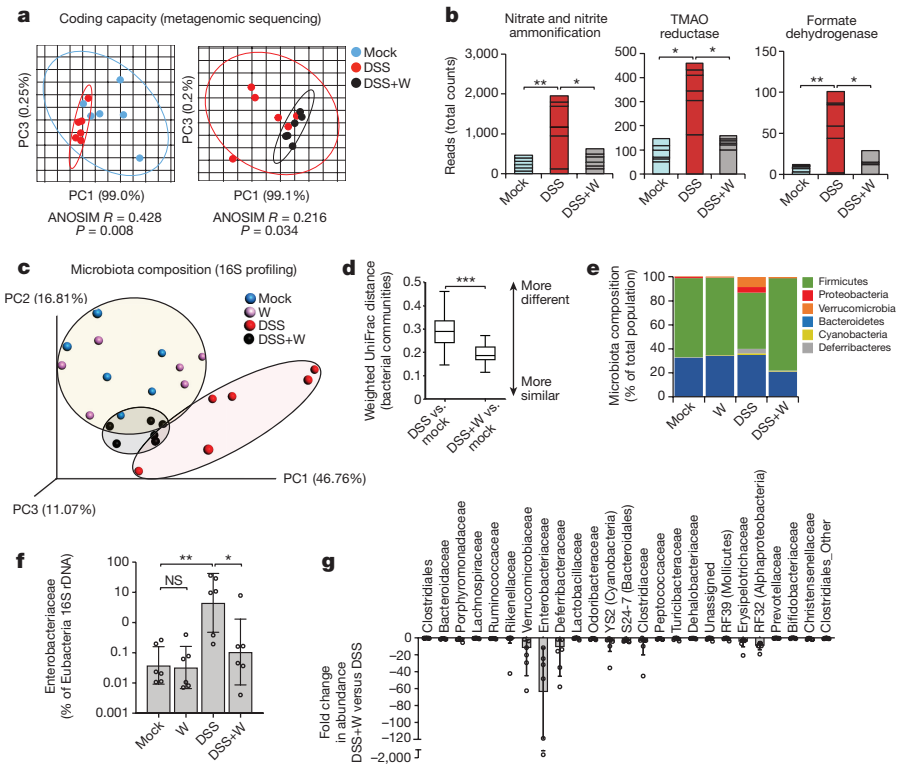

Figure 2 | Effect of tungstate treatment on composition of gut bacterial community and metabolic landscape. DNA extracted from the caecal contents of C57BL/6 mice ($n = 6$ per group) receiving the indicated treatments was analysed by metagenomic sequencing and 16S profiling. **a**, Principal coordinates analysis (PCoA) plots and analysis of similarity (ANOSIM) of the predicted coding capacity. Ellipses in **a** denote 95% confidence intervals. **b**, Tallied metagenomic reads mapped to anaerobic respiration and formate utilization pathways. **c**, PCoA of the microbiota composition (weighted UniFrac distances). **d**, Box-and-whisker plot (boxes show median, first and third quatiles, whisker denotes minimum to maximum range) of intercommunity β-diversity determined by weighted 16S UniFrac distances. **e**, Phylum-level microbiota composition. **f**, Abundance of Enterobacteriaceae quantified by qPCR. **g**, Changes in the population size of the 25 most abundant operational taxonomic units as the result of tungstate administration in the DSS-induced-colitis model. Unless otherwise noted, data are shown as geometric mean and geometric s.d.

tungsten-mediated manipulation of the gut microbiota could ameliorate gut inflammation. Alternatively, one could hypothesize that tungstate exerted anti-inflammatory effects directly on the host immune system. To test the latter hypothesis, we treated groups of germ-free C57BL/6 mice with DSS and tungstate or DSS alone for nine days and analysed the intestinal inflammatory responses. Treatment of germ-free mice with DSS resulted in moderate inflammation compared to germ-free control mice. Concomitant administration of tungstate did not

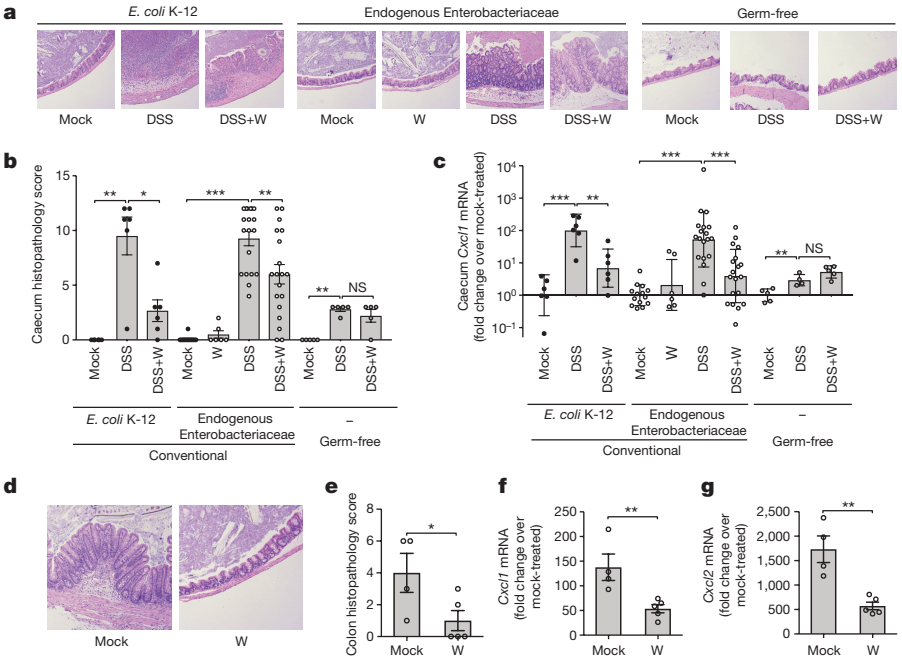

Figure 3 | Influence of tungstate treatment on mucosal inflammation. **a**–**c**, Conventionally raised C57BL/6 mice, treated with DSS or DSS and tungstate for four days, were inoculated with *E. coli* K-12 and samples were analysed after five days. C57BL/6 mice with a naive microbiota (including endogenous Enterobacteriaceae) or germ-free C57BL/6 mice were treated similarly with tungstate, DSS or DSS plus tungstate. *E. coli* K-12: $n = 6$ for all groups. Endogenous Enterobacteriaceae: mock, $n = 14$; W, $n = 6$; DSS, $n = 19$; DSS+W, $n = 19$. Germ-free: $n = 5$ for all groups (except in **c**; DSS, $n = 4$). **a**, Representative images of haematoxylin and eosin-stained caecal sections. **b**, Cumulative histopathology score for the caecum; data are shown as mean and s.e.m., and each dot represents one animal. **c**, Transcription of *Cxcl1* (also known as *KC*) in the caecal mucosa, determined by RT–qPCR. **d**–**g** Groups of *Il10*$^{-/-}$ mice were inoculated orally with *E. coli* NC101. Animals received piroxicam-fortified diet or piroxicam-fortified diet plus tungstate in drinking water for two weeks; mock, $n = 4$; W, $n = 5$. **d**, Representative images of haematoxylin and eosin-stained colonic sections. **e**, Cumulative histopathology score for the colon; data are shown as mean and s.e.m., and each dot represents one animal. **f**, **g**, Abundance of *Cxcl1* (**f**) and *Cxcl2* (**g**) mRNA in the colonic mucosa, determined by RT–qPCR. Unless otherwise noted, data are shown as geometric mean and geometric s.d.

interfere with the induction of this response, indicating that tungsten limits intestinal inflammation by manipulating the gut microbiota (Fig. 3a–c, Extended Data Fig. 2c, d). Tungstate had no observable effect on pro-inflammatory responses or cellular resistance to DSS injury in cultured cells (Extended Data Fig. 8b–d). Therapeutic administration of tungstate after the onset of inflammation was sufficient to inhibit molybdenum-cofactor-dependent processes in *E. coli* Nissle 1917 (Extended Data Fig. 8e, f), supporting the hypothesis that the effect of tungsten on microbial populations was not due to tungstate interfering with the induction of DSS-induced inflammation. Collectively, these data suggest that tungsten limits gut inflammation through manipulation of the mouse gut microbiota.

A subset of people with inflammatory bowel disease exhibit changes in the composition of their gut microbiota that include increased abundance of Enterobacteriaceae family members[1]. We humanized the gut of germ-free mice with gut microbiota from patients with active flares. To model intestinal inflammation, groups of mice were treated with either DSS alone or DSS and tungstate, and housed separately. Administration of tungstate reduced the intestinal Enterobacteriaceae load and decreased markers of mucosal inflammation (Extended Data Fig. 4i–m), thus providing evidence that the effect of tungsten is not unique to mouse microbiota.

An imbalance in the gut-associated microbial community may underlie many human diseases, but current approaches to treating dysbiosis lack the sophistication needed to restore a balanced community *in situ*. Administration of antibiotics broadly reduces numbers of many members of the gut microbiota without discriminating between beneficial and potentially harmful microbes. In some instances, removal of potentially harmful members of the community can lead to a beneficial outcome[14–16]. However, removal of beneficial microbes can lead to pathogen expansion[2,17] or increased bowel irritability[18], thereby adversely affecting the host. Commensal Enterobacteriaceae contribute to resistance to colonization by enteric pathogens by competing for critical nutrients[19,20]. Oral administration of probiotic *E. coli* Nissle 1917 is effective in maintaining remission in patients with ulcerative colitis[21], and microcins produced by *E. coli* Nissle 1917 suppress the growth of pathogenic bacteria[22]. Thus, it might be preferable to control the population size of commensal Enterobacteriaceae in the gut microbiome than to remove them entirely. In contrast to broad-spectrum antibiotics, tungstate treatment of the dysbiotic microbiota allows selective control of bacterial populations, such as Enterobacteriaceae, that rely on molybdenum-cofactor-dependent processes. Because these molybdenum-cofactor-dependent processes operate only during gut inflammation[11], tungsten treatment acts only on the enterobacterial population in the disease state, and does not eliminate Enterobacteriaceae from the ecosystem during homeostatic conditions. Our work identifies molybdenum-cofactor-dependent processes as a target for controlling disease-specific aspects of the microbiota composition. Furthermore, our results provide experimental evidence that this rationally designed microbiome editing approach can improve dysbiosis-associated mucosal inflammation.

Online Content Methods, along with any additional Extended Data display items and Source Data, are available in the online version of the paper; references unique to these sections appear only in the online paper.

Received 9 November 2015; accepted 24 November 2017.
Published online 3 January 2018.

1. Frank, D. N. *et al.* Molecular-phylogenetic characterization of microbial community imbalances in human inflammatory bowel diseases. *Proc. Natl Acad. Sci. USA* **104,** 13780–13785 (2007).
2. Lupp, C. *et al.* Host-mediated inflammation disrupts the intestinal microbiota and promotes the overgrowth of Enterobacteriaceae. *Cell Host Microbe* **2,** 119–129 (2007).
3. Garrett, W. S. *et al.* Enterobacteriaceae act in concert with the gut microbiota to induce spontaneous and maternally transmitted colitis. *Cell Host Microbe* **8,** 292–300 (2010).
4. Mshvildadze, M. *et al.* Intestinal microbial ecology in premature infants assessed with non-culture-based techniques. *J. Pediatr.* **156,** 20–25 (2010).
5. Vujkovic-Cvijin, I. *et al.* Dysbiosis of the gut microbiota is associated with HIV disease progression and tryptophan catabolism. *Sci. Transl. Med.* **5,** 193ra91 (2013).
6. Raetz, M. *et al.* Parasite-induced TH1 cells and intestinal dysbiosis cooperate in IFN-γ-dependent elimination of Paneth cells. *Nat. Immunol.* **14,** 136–142 (2013).
7. Winter, S. E., Lopez, C. A. & Bäumler, A. J. The dynamics of gut-associated microbial communities during inflammation. *EMBO Rep.* **14,** 319–327 (2013).
8. Shin, N. R., Whon, T. W. & Bae, J. W. Proteobacteria: microbial signature of dysbiosis in gut microbiota. *Trends Biotechnol.* **33,** 496–503 (2015).
9. Garrett, W. S. *et al.* Communicable ulcerative colitis induced by T-bet deficiency in the innate immune system. *Cell* **131,** 33–45 (2007).
10. Elinav, E. *et al.* NLRP6 inflammasome regulates colonic microbial ecology and risk for colitis. *Cell* **145,** 745–757 (2011).
11. Hughes, E. R. *et al.* Microbial respiration and formate oxidation as metabolic signatures of inflammation-associated dysbiosis. *Cell Host Microbe* **21,** 208–219 (2017).
12. Winter, S. E. *et al.* Host-derived nitrate boosts growth of *E. coli* in the inflamed gut. *Science* **339,** 708–711 (2013).
13. Gates, A. J. *et al.* Properties of the periplasmic nitrate reductases from *Paracoccus pantotrophus* and *Escherichia coli* after growth in tungsten-supplemented media. *FEMS Microbiol. Lett.* **220,** 261–269 (2003).
14. Hans, W., Schölmerich, J., Gross, V. & Falk, W. The role of the resident intestinal flora in acute and chronic dextran sulfate sodium-induced colitis in mice. *Eur. J. Gastroenterol. Hepatol.* **12,** 267–273 (2000).
15. Rutgeerts, P. *et al.* Controlled trial of metronidazole treatment for prevention of Crohn's recurrence after ileal resection. *Gastroenterology* **108,** 1617–1621 (1995).
16. Prantera, C. *et al.* An antibiotic regimen for the treatment of active Crohn's disease: a randomized, controlled clinical trial of metronidazole plus ciprofloxacin. *Am. J. Gastroenterol.* **91,** 328–332 (1996).
17. Stecher, B. *et al. Salmonella enterica* serovar Typhimurium exploits inflammation to compete with the intestinal microbiota. *PLoS Biol.* **5,** 2177–2189 (2007).
18. Collins, S., Verdu, E., Denou, E. & Bercik, P. The role of pathogenic microbes and commensal bacteria in irritable bowel syndrome. *Dig. Dis.* **27** (Suppl 1), 85–89 (2009).
19. Kamada, N. *et al.* Regulated virulence controls the ability of a pathogen to compete with the gut microbiota. *Science* **336,** 1325–1329 (2012).
20. Brugiroux, S. *et al.* Genome-guided design of a defined mouse microbiota that confers colonization resistance against *Salmonella enterica* serovar Typhimurium. *Nat. Microbiol.* **2,** 16215 (2016).
21. Kruis, W. *et al.* Maintaining remission of ulcerative colitis with the probiotic *Escherichia coli* Nissle 1917 is as effective as with standard mesalazine. *Gut* **53,** 1617–1623 (2004).
22. Sassone-Corsi, M. *et al.* Microcins mediate competition among Enterobacteriaceae in the inflamed gut. *Nature* **540,** 280–283 (2016).

Supplementary Information is available in the online version of the paper.

Acknowledgements This work was supported by NIH grants AI112445 (A.J.B.), AI118807 (S.E.W.), AI128151 (S.E.W.), DK070855 (L.V.H.), DK102436 (B.A.D.) and 5K12HD-068369 (L.S.-D.), Welch Foundation grants I-1858 (S.E.W.) and I-1874 (L.V.H.), American Cancer Society Research Scholar Grant MPC-130347 (S.E.W.) and a Crohn's and Colitis Foundation of America postdoctoral fellowship no. 454921 (W.Z.). Work in the L.V.H. laboratory is supported by the Howard Hughes Medical Institute. The funders had no role in study design, data collection and interpretation, or the decision to submit the work for publication. Any opinions, findings, and conclusions or recommendations expressed in this material are those of the authors and do not necessarily reflect the views of the funders. We thank B. Sartor for the *E. coli* NC101 strain.

Author Contributions W.Z., M.G.W., L.S., L.B., E.d.L.R., R.P.W., E.R.H, C.A.L. and C.C.G. performed and analysed nitrate reductase activity, *in vitro* bacterial competitive growth, NF-κB induction, DSS cytotoxity experiments and experiments involving conventionally raised C57BL/6 mice. M.G.W., L.S. and E.R.H. performed *Il10*$^{-/-}$ mouse experiments. W.Z. and M.G.W. performed inflammation analysis. C.L.B., M.G.W., L.S. and W.Z. performed germ-free-mouse experiments. B.A.D. and W.Z. analysed 16S and metagenomic data. M.X.B. analysed the histopathology. L.S.-D. and K.H.-H. contributed to humanized mouse experiments. L.S. and S.E.W. performed metabolite quantification. W.Z., Ç.T., A.Y.K., E.B., L.V.H., A.J.B. and S.E.W. designed the experiments, interpreted the data and wrote the manuscript with contributions from all authors.

Author Information Reprints and permissions information is available at www.nature.com/reprints. The authors declare competing financial interests: details are available in the online version of the paper. Readers are welcome to comment on the online version of the paper. Publisher's note: Springer Nature remains neutral with regard to jurisdictional claims in published maps and institutional affiliations. Correspondence and requests for materials should be addressed to A.J.B. (ajbaumler@ucdavis.edu) or S.E.W. (Sebastian.Winter@UTSouthwestern.edu).

Reviewer Information *Nature* thanks C. Elson, M. Fischbach and the other anonymous reviewer(s) for their contribution to the peer review of this work.

METHODS

Bacterial strains. The *E. coli*, *Proteus*, and *E. cloacae* strains used in this study are listed in Supplementary Table 1. All strains were routinely grown aerobically in LB broth (10 g l^{-1} tryptone, 5 g l^{-1} yeast extract, 10 g l^{-1} NaCl) or on LB agar plates (10 g l^{-1} tryptone, 5 g l^{-1} yeast extract, 10 g l^{-1} NaCl, 15 g l^{-1} agar) at 37 °C. When appropriate, antibiotics were added to the medium at the following concentrations: 30 μg ml^{-1} chloramphenicol, 100 μg ml^{-1} carbenicillin, 50 μg ml^{-1} kanamycin.

Plasmids. All primers and plasmids are listed in Supplementary Tables 2 and 3. pWZ5 was constructed with standard molecular cloning techniques[23] using the Gibson Assembly Cloning Kit (New England Biolab) according to the recommendations of the manufacturer. The flanking regions of the *moaA* gene from the *E. coli* strain NRG857c were amplified and ligated into pGP706 to make pWZ5. Plasmid inserts were verified by Sanger sequencing.

Construction of mutants by allelic exchange. pWZ5 was propagated in DH5α λ*pir* and conjugated into the *E. coli* strains NRG857c or NC101 using S17-1 λ*pir* as the conjugative donor strain. Exconjugants that had the suicide plasmid integrated into the recipient chromosome (single crossover) were recovered on LB plates containing appropriate antibiotics. Sucrose plates (8 g l^{-1} nutrient broth base, 5% sucrose, 15 g l^{-1} agar) were used to select for the second crossover event, thus creating WZ12 and WZ245, respectively. Deletion of the target gene was confirmed by PCR.

Anaerobic growth assays. Anaerobic growth assays were performed in mucin broth. Mucin broth contained hog mucin (Sigma–Aldrich) at a final concentration of 0.5% (w/v) in no-carbon E medium[24] and was supplemented with trace elements[25]. Sodium formate, sodium nitrate, DMSO and trimethylamine-N-oxide (TMAO, Sigma–Aldrich) were added to a final concentration of 40 mM, in the absence or presence of sodium tungstate (Sigma–Aldrich) at the indicated final concentrations. A volume of 2 ml of mucin broth was inoculated with the indicated strains at a concentration of 1×10^4 colony-forming units (CFU) per ml and incubated anaerobically (Bactron EZ Anaerobic Chamber, Sheldon Manufacturing) for 18 h at 37 °C. Bacterial numbers were counted as described[12].

DSS-induced-colitis model and sodium tungstate treatment. All experiments involving mice were approved by the Institutional Animal Care and Use Committee at UT Southwestern Medical Center (APN#T-2013-0159) and UC Davis (APN#16196). Studies involving animals were performed with compliance to all relevant ethical regulations. Female 9–12-week-old C57BL/6J wild-type mice were obtained from Jackson Laboratory (Bar Harbour) and bred at UT Southwestern (essentially devoid of endogenous Enterobacteriaceae) or Charles River Laboratories (Morrisville) (harbouring endogenous Enterobacteriaceae), as indicated. Mice were randomly assigned into cages before the experiment. The drinking water was replaced with either filter-sterilized water (mock treatment), a filter-sterilized solution of 0.2% (w/v) sodium tungstate (Sigma), a filter-sterilized solution of 2% or 3% (w/v) DSS (relative molecular mass 36,000–50,000; MP Biomedicals) in water, or a filter-sterilized solution of DSS and 0.2% (w/v) sodium tungstate. In one experiment, tungsten was administered in a sodium tungstate-fortified diet (1,000 parts per million (p.p.m.)). At the indicated time points, animals were inoculated orally with either 0.1 ml LB broth or 0.1 ml LB broth containing 1×10^9 CFU *E. coli*, or remained uninfected. In the competitive colonization experiments, mice were inoculated with 5×10^8 CFU of each *E. coli* or *E. cloacae* strain. One day before the end of the experiment, the drinking water was switched to regular, filter-sterilized water for 24 h to reduce the amount of DSS present in the samples. After euthanization, colonic and caecal tissue were collected, flash frozen and stored at −80 °C for subsequent mRNA and protein expression analysis. Faecal material, caecal content, and colonic content were collected in sterile PBS and the bacterial loads for the *E. coli* strains or Enterobacteriaceae were quantified by plating serial tenfold dilutions on LB plates supplemented with appropriate antibiotics or MacConkey agar plates, respectively. *E. coli* NC101 and Nissle 1917 strains were differentially marked with the low-copy number plasmids pWSK29 and pWSK129 to facilitate bacterial recovery from biological samples[12]. For the competitive colonization experiments involving NRG857c, animals were inoculated with an equal mixture of the NRG857c Δ*lacZ* mutant (LB33) and the Δ*moaA* mutant (WZ12) as described above. The bacterial load in the luminal content of the indicated organs was determined by plating serial tenfold dilutions on LB plates supplemented with the appropriate antibiotics and 40 mg l^{-1} 5-bromo-4-chloro-3-indolyl-β-D-galactopyranoside. Germ-free C57BL/6 mice were maintained in plastic gnotobiotic isolators on a 12-h light cycle. DSS-mediated colitis was induced in 8–12-week-old germ-free mice, following the protocol described above.

Piroxicam-accelerated colitis model in conventional *Il10*$^{-/-}$ mice. Conventional *Il10*$^{-/-}$ mice (7–12 weeks old, males only) on a C57BL/6 background were randomly assigned into cages before oral inoculation with 1×10^9 CFU of mouse AIEC NC101. Regular mouse chow was replaced with piroxicam-fortified diet (100 p.p.m.; Teklad custom research diets, Envigo) and changed daily. Drinking water was replaced with either filter-sterilized water (mock treatment) or a filter-sterilized solution of 0.2% (w/v) sodium tungstate. After 14 days, mice were euthanized and the samples were collected as described above.

Faecal transplant into gnobiotic mice. All procedures involving human subjects were reviewed and approved by the institutional review board at the University of Texas Southwestern Medical Center (IRB#112010-130). Studies involving human samples were performed with compliance to all relevant ethical regulations. Written informed consent was obtained from all participants or parents or legal guardians of participating minors. Except for E.B. and S.F.-D., none of the investigators handling the samples had access to personally identifiable information. Patients were considered for faecal donation if they had an established diagnosis of inflammatory bowel disease, had active disease at the time of collection and were free from antibiotic use over the past three months. Characteristics of patients from whom samples were taken are summarized in Supplementary Table 4. Human faecal samples were obtained during colonoscopy by direct endoscopic aspiration of faecal contents from patients with active colonic disease. A total of 10 ml of liquid faecal material was collected from each patient and aliquoted into 1-ml cryovials. The samples were then snap-frozen in liquid nitrogen and stored at −80 °C until use.

Germ-free Swiss–Webster mice (7–12 weeks old, mix of male and female) were maintained in plastic gnotobiotic isolators on a 12-h light cycle. Mice were randomized, paired and orally gavaged with endoscopy samples from the patients listed in the table at the end of this section. Colonization was allowed to proceed for three days before mice received DSS or DSS plus sodium tungstate for seven days. Mice were euthanized and the samples were collected as described above.

16S RNA pyrosequencing and analysis. Caecal contents were collected and DNA was extracted from faecal samples using the MoBio PowerFecal kit (MoBio Laboratories) according to the recommendations of the manufacturer. The extracted DNA was subjected to KCl precipitation to remove residual DSS contaminants. In brief, DNA was incubated with excess KCl on ice to precipitate DSS. The samples were then cleared by centrifugation and the resulting supernatant was subsequently subjected to ethanol precipitation to recover the DNA. The purified DNA was subjected to paired end library construction to facilitate assemblies and longer accurate reads. The 16S rRNA coding sequences used to identify the bacteria were amplified using primers 515F and 806R that flank the V3–V4 hypervariable region, and barcoded before pyrosequencing. The barcoded amplicons were purified and quantified on an Invitrogen Qubit system (Life technology). Libraries were sequenced using an Illumina MiSeq system (Illumina). 16S-sequencing data was subjected to a standard workflow for processing and quality assessment of the raw 16S-sequence data and the downstream phylogenetic analysis. The pipeline consists of an initial customized Linux-based command script for trimming, demultiplexing and quality filtering the raw paired end-sequence data generated by the Illumina system. Sequence alignment, operational taxonomic units (OTUs) picking against the Greengenes reference collection, clustering, phylogenetic and taxonomic profiling, permutational multivariate analysis of variance (PERMANOVA), and the analysis of beta diversity (principle component analysis) on the demultiplexed sequences were performed with the Quantitative Insights into Microbial Ecology (QIIME) open source software package[26].

Metagenomics. Groups of randomized Charles River C57BL/6 mice were treated as described in Extended Data Fig. 2b. Sample collection, shotgun metagenomics sequencing and data analysis were performed as previously described[11].

Reads that mapped to the SEED database were exported from MEGAN5 into BIOM tables, which were subjected to analysis of similarity (ANOSIM) in Qiime[26] and principal component analysis (PCA) using STAMP[27]. To map reads to bacterial metabolic genes, a total of 100 of each of the butyrate production operons (*bcdAB, but* and *ato*) and succinate dehydrogenase operons (*sdhABC*) were downloaded from the KEGG database. Sequences were clustered to remove redundancy using cdhit-est[28,29] with a sequence identity threshold of 0.9. Paired end reads were mapped to these gene clusters using the BBmap tool with the following settings: 'qtrim = lr, minid = 0.90, ambig = random, covstats = true'. Coverage statistics for each gene cluster were tallied from the percentage of unambiguous and ambiguous mapped reads and used to determine the absolute number of reads that mapped to a particular gene set. A similar strategy was used to map reads to fumarate respiration and butyrate production pathways.

Abundance of Enterobacteriaceae. The relative abundance of endogenous Enterobacteriaceae as part of the bacterial microbiota was analysed as described previously[30–32]. In brief, the caecum or colon content was extracted using the PowerFecal DNA Isolation Kit (MoBio Laboratories) according to the manufacturer's instructions, and the resulting DNA was further purified using the KCl method as described above. A 2-μl sample of the bacterial DNA was used as the template for SYBR Green-based real-time PCR reactions as described above. The gene copy number in the sample was determined based on a standard curve generated using

pSW321 and pSW196 as previously described[33]. The primers used are listed in Supplementary Table 2. The fraction of Enterobacteriaceae as part of the entire bacterial population for each sample was calculated by dividing the gene-copy number of the *Enterobacteriacaea* by the gene-copy number determined using the eubacterial primers.

Quantification of mRNA levels in intestinal tissue. The relative transcription levels of mRNAs for iNOS, CXCL1, CXCL2, IL-17, IL-6, IFN-γ, LCN2 and TNF-α, encoded by the *Nos2*, *Cxcl1*, *Cxcl2, Il17, Il6*, *Ifng*, *Lcn2* and *Tnf* genes, respectively, were determined by qRT–PCR as described previously[31]. In brief, colonic or caecal tissue was homogenized in a Mini Beadbeater (Biospec Products) and RNA was extracted using the TRI-reagent method (Molecular Research Center). To remove residual DSS contaminants, RNA was further purified using the Dynabeads mRNA Direct Kit (Life Technologies) per the manufacturer`s instructions. cDNA was generated with TaqMan reverse-transcription reagents (Life Technologies). Real-time PCR was performed using SYBR Green (Life Technologies), and data were acquired in a QuantStudio 6 Flex instrument (Life Technologies) and analysed using the comparative C_t method. The primers listed in Supplementary Table 2 were added at a final concentration of 250 nM. Target-gene transcription of each sample was normalized to the respective levels of *Gapdh* mRNA.

Histopathology. Mouse caecal and colonic tissue was fixed in phosphate-buffered formalin and 5-μm sections of the tissue were stained with haematoxylin and eosin. The fixed and stained sections were blinded and evaluated by an experienced veterinary pathologist according to the criteria described previously[12]. Images were taken at a magnification of 10×, and the contrast for the images was uniformly (linear) adjusted using Adobe Photoshop CC.

Measurement of succinate and butyrate concentrations in bacterial culture using GC–MS. Bacterial cultures were cleared by centrifugation at 13,200*g* at 4 °C for 30 min and then passed through a 0.22-μm filter. The supernatant was dried using a SpeedVac concentrator. The pellet was then dissolved in pyridine at 80 °C for 20 min before derivatization with *n-tert*-butyldimethylsilyl-*n*-methyltrifluoroacetamide with 1% t-BDMCS sylilation reagent (Cerilliant) at 80 °C for 1 h. Derivatized samples were transferred to autosampler vials for gas chromatography–mass spectrometry (GC–MS) analysis (Shimadzu, TQ8040). The injection temperature was 250 °C and the injection split ratio was set to 1:100 or 1:1,000 with an injection volume of 1 μL. The gas chromatography oven temperature started at 130 °C for 4 min, rising to 230 °C at 4 °C min^{-1}, and to 280 °C at 20 °C min^{-1} with a final hold at this temperature for 2 min. The gas chromatography flow rate of the helium carrier gas was kept constant at a linear velocity of 50 cm s^{-1}. The column used was a 30 m × 0.25 mm × 0.25 μm Rtx-5Sil MS (Shimadzu). The interface temperature was 300 °C. The electron-impact ion-source temperature was 200 °C, with 70 V ionization voltage and 150 μA current. To measure succinate, Q3 scans (range of 50–500 *m*/*z*, 1000 *m*/*z* per second) were first performed to determine the retention time for succinate and succinate-2,2,3,3-d_4 (CDN Isotopes), which was 11.0 and 10.9 min respectively. Multiple-reaction-monitoring mode was then used (target ion *m*/*z* 289→147, reference ion *m*/*z* 331→189) to measure succinate quantitatively. To measure butyrate, Q3 scans were performed as described above, and the retention time for butyrate and butyrate-d_7 (CDN Isotopes) was 6.1 and 6.2 min, respectively. Q3-selected ion monitoring (single-quadrupole mode) with an event time of 0.05 s was performed to quantitatively measure butyrate. The target and reference (qualifier) ions for butyrate were *m*/*z* = 145 and *m*/*z* = 75, respectively; target and reference ions for deuterated butyrate were *m*/*z* = 152 and *m*/*z* = 76.

Strain isolation and identification. Tenfold serial dilutions of the faecal content of C57BL/6 mice (Charles River) were plated on MacConkey agar (10 g l^{-1} pancreatic digest of gelatin, 3 g l^{-1} peptone, 10 g l^{-1} lactose, 1.5 g l^{-1} bile salts, 5 g l^{-1} sodium chloride, 13.5 g l^{-1} agar, 30 mg l^{-1} neutral red, 1 mg l^{-1} crystal violet) and incubated aerobically at 37 °C overnight. To isolate mouse–commensal *E. coli* and *Proteus* strains, single colonies were isolated and identified using the EnteroPluri Test (Liofilchem) per the manufacturer`s recommendations.

Nitrate reductase activity assays. Overnight cultures of *E. coli* or *Proteus* strains were diluted 1:100 in fresh LB broth containing 40 mM sodium nitrate to induce the expression of nitrate reductases, in the presence or absence of sodium tungstate at the indicated concentrations. Cultures were incubated aerobically for 3 h at 37 °C and the relative nitrate reductase activity was measured as described previously[34]. The experiment was repeated three times and representative results are shown.

NF-κB activation in epithelial cells. HeLa57A cells, stably transfected with an NF-κB–luciferase reporter construct[35,36], were maintained in Dulbecco's modified Eagle's medium (DMEM) containing 10% fetal calf serum at 37 °C in a 5% CO_2 atmosphere. For the NF-κB activation assays, cells were seeded in a 48-well plate to reach 80% confluency within 24 h. Cells were treated with 0.1, 1 or 10 ng ml^{-1} of phorbol 12-myristate 13-acetate (PMA, dissolved in DMSO) or DMSO alone. At the same time, sodium tungstate with a final concentration of 0.02% or 0.002% (w/v) in water was added to the cells. After 5 h, cells were washed in DPBS and lysed in 0.1 ml of reporter lysis buffer (Promega). Firefly luciferase activity was measured with a commercial luciferase assay system (Promega). The experiment was repeated three times and representative results are shown. HeLa57A cells were generated by R. T. Hay (University of Dundee). These cells have not been authenticated or tested for mycoplasma contamination.

LDH-release assay. The MODE-K cell line was maintained in DMEM (Sigma) supplemented with 10% FBS at 37 °C in 5% CO_2. Bone-marrow-derived macrophages (BMDMs) were differentiated from bone-marrow cells collected from femurs and tibias of SPF C57BL/6 mice. In brief, bone-marrow cells were collected with 10 ml cold RPMI-1640 medium (Sigma) and then pelleted at 1,000 r.p.m. for 5 min at 25 °C. The cells were resuspended in BMM medium (RPMI-1640 supplemented with 10% heat-inactivated FBS, 1 mM glutamine, 1% antibiotics–antimycotics, and 30% L-cell conditioned medium) and allowed to differentiate for seven days. MODE-K experiments were performed in triplicate. Plates were seeded with cells to a final confluency of 80% before treatment. Two days after seeding, MODE-K cells were treated for 24 h with 2–4% DSS (Alfa Aesar), with and without 0.002–0.2% sodium tungstate dihydrate (Sigma). For BMDM experiments, plates were seeded with 1×10^5 cells per well for 48 h. After 24 h the medium was replaced with RPMI supplemented with 2% FBS and glutamine. On the day of the experiment, culture medium was replaced with medium supplemented with 4 or 6% DSS, with and without 0.2% sodium tungstate dehydrate, for 24 h. Cytotoxicity was determined using the LDH-release assay CytoTox 96 non-radioactive cytotoxicity assay (Promega), per the manufacturer's recommendations. Absorbance readings were corrected based on the absorbance of the medium alone. Five-minute treatment with 10% Triton X-100 was used as the total LDH-release control. The experiment was repeated three times, and representative results are shown. MODE-K cells were generated by D. Kaiserlian (Institut Pasteur de Lyon). These cells have not been authenticated or tested for mycoplasma contamination.

Statistics and reproducibility. No statistical methods were used to predetermine sample size. The investigators were not blinded to allocation during experiments and outcome assessment, except for histology analysis. Nitrate reductase activities, fold changes in mRNA levels, competitive indices, relative abundance of Enterobacteriaceae and bacterial numbers were transformed logarithmically and the statistical significance of differences between groups was determined using a two-sided Student's *t*-test or PERMANOVA (using distance matrices). Cumulative histopathology scores were analysed using the Mann–Whitney *U* test. Details regarding the statistics of each experiment are reported in Supplementary Table 5.

Data availability. The bacterial 16S-ribosomal DNA and metagenomics-sequencing reads generated and analysed during the current study are available at the European Bioinformatics Institute repository under accession numbers PRJEB15095 and PRJEB19192. All data generated or analysed during this study are included in this published article (and its Supplementary Information files).

23. Sambrook, J., Fritsch, E. F. & Maniatis, T. *Molecular Cloning* 2nd edn (Cold Spring Harbor Laboratory Press, 1989).
24. Davis, R. W., Roth, J. R. & Botstein, D. *Advanced Bacterial Genetics* (Cold Spring Harbor Laboratory Press, 1980).
25. Price-Carter, M., Tingey, J., Bobik, T. A. & Roth, J. R. The alternative electron acceptor tetrathionate supports B12-dependent anaerobic growth of *Salmonella enterica* serovar Typhimurium on ethanolamine or 1,2-propanediol. *J. Bacteriol.* **183,** 2463–2475 (2001).
26. Caporaso, J. G. *et al.* QIIME allows analysis of high-throughput community sequencing data. *Nat. Methods* **7,** 335–336 (2010).
27. Shavit, Y., Hamey, F. K. & Lio, P. FisHiCal: an R package for iterative FISH-based calibration of Hi-C data. *Bioinformatics* **30,** 3120–3122 (2014).
28. Li, W. & Godzik, A. Cd-hit: a fast program for clustering and comparing large sets of protein or nucleotide sequences. *Bioinformatics* **22,** 1658–1659 (2006).
29. Fu, L., Niu, B., Zhu, Z., Wu, S. & Li, W. CD-HIT: accelerated for clustering the next-generation sequencing data. *Bioinformatics* **28,** 3150–3152 (2012).
30. Barman, M. *et al.* Enteric salmonellosis disrupts the microbial ecology of the murine gastrointestinal tract. *Infect. Immun.* **76,** 907–915 (2008).
31. Winter, S. E. *et al.* Contribution of flagellin pattern recognition to intestinal inflammation during *Salmonella enterica* serotype Typhimurium infection. *Infect. Immun.* **77,** 1904–1916 (2009).
32. Winter, S. E. *et al.* Gut inflammation provides a respiratory electron acceptor for *Salmonella*. *Nature* **467,** 426–429 (2010).
33. Bacchetti De Gregoris, T., Aldred, N., Clare, A. S. & Burgess, J. G. Improvement of phylum- and class-specific primers for real-time PCR quantification of bacterial taxa. *J. Microbiol. Methods* **86,** 351–356 (2011).
34. Stewart, V. & Parales, J. Jr. Identification and expression of genes *narL* and *narX* of the *nar* (nitrate reductase) locus in *Escherichia coli* K-12. *J. Bacteriol.* **170,** 1589–1597 (1988).
35. Rodriguez, M. S., Thompson, J., Hay, R. T. & Dargemont, C. Nuclear retention of IκBα protects it from signal-induced degradation and inhibits nuclear factor κB transcriptional activation. *J. Biol. Chem.* **274,** 9108–9115 (1999).
36. Keestra, A. M. *et al.* A *Salmonella* virulence factor activates the NOD1/NOD2 signaling pathway. *MBio* **20,** e00266–11 (2011).

37. Eaves-Pyles, T. *et al. Escherichia coli* isolated from a Crohn's disease patient adheres, invades, and induces inflammatory responses in polarized intestinal epithelial cells. *Int. J. Med. Microbiol.* **298,** 397–409 (2008).
38. Kim, S. C. *et al.* Variable phenotypes of enterocolitis in interleukin 10-deficient mice monoassociated with two different commensal bacteria. *Gastroenterology* **128,** 891–906 (2005).
39. Pal, D., Venkova-Canova, T., Srivastava, P. & Chattoraj, D. K. Multipartite regulation of *rctB*, the replication initiator gene of *Vibrio cholerae* chromosome II. *J. Bacteriol.* **187,** 7167–7175 (2005).
40. Simon, R., Priefer, U. & Puhler, A. A broad host range mobilization system for *in vivo* genetic engineering: transposon mutagenesis in gram negative bacteria. *Nat. Biotechnol.* **1,** 784–791 (1983).
41. Overbergh, L. *et al.* The use of real-time reverse transcriptase PCR for the quantification of cytokine gene expression. *J. Biomol. Tech.* **14,** 33–43 (2003).
42. Godinez, I. *et al.* T cells help to amplify inflammatory responses induced by *Salmonella enterica* serotype Typhimurium in the intestinal mucosa. *Infect. Immun.* **76,** 2008–2017 (2008).
43. Wilson, R. P. *et al.* The Vi-capsule prevents Toll-like receptor 4 recognition of *Salmonella*. *Cell. Microbiol.* **10,** 876–890 (2008).
44. Wang, R. F. & Kushner, S. R. Construction of versatile low-copy-number vectors for cloning, sequencing and gene expression in *Escherichia coli*. *Gene* **100,** 195–199 (1991).

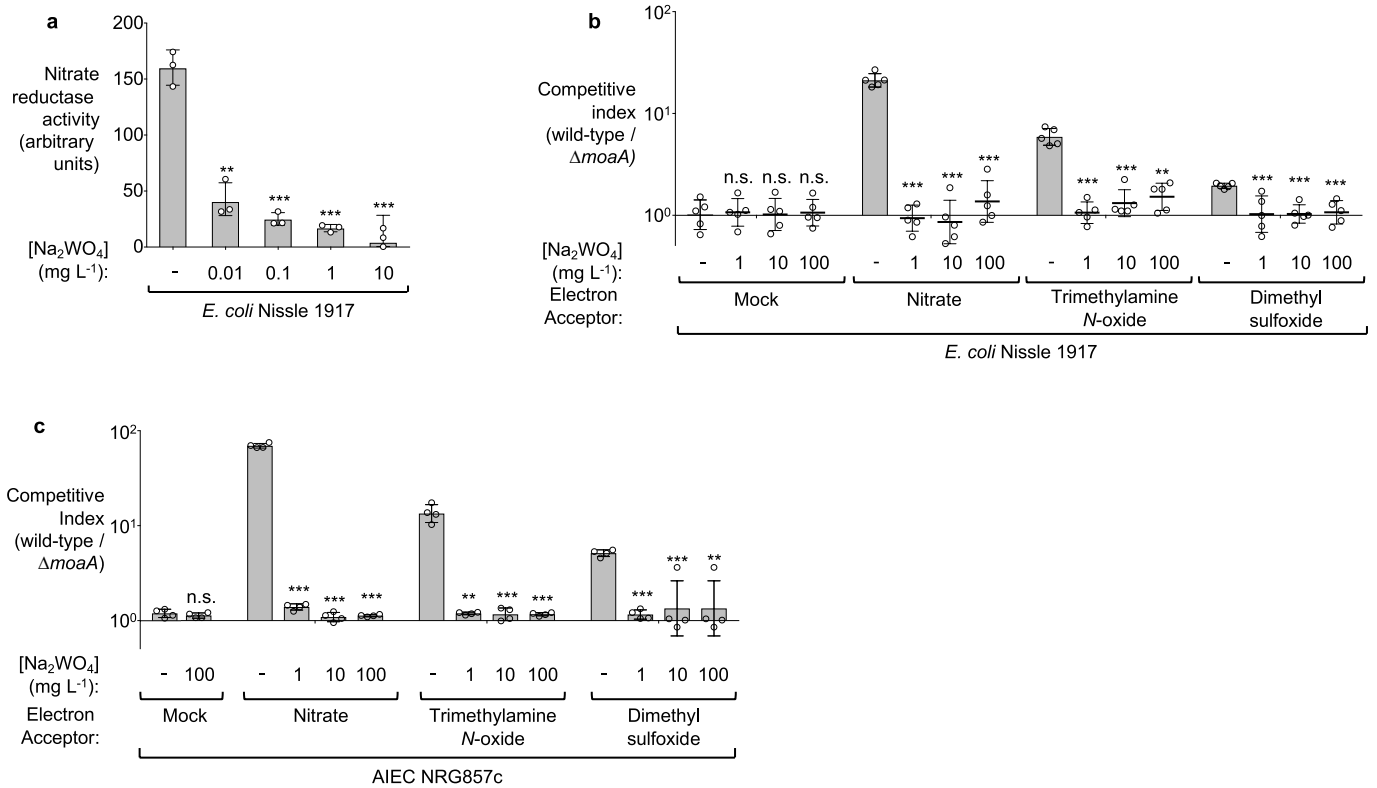

Extended Data Figure 1 | Effect of tungstate on anaerobic respiration *in vitro*. **a**, Nitrate reductase activity of *E. coli* Nissle 1917 measured in medium supplemented with sodium nitrate and the indicated concentrations of sodium tungstate. **b**, Competitive growth of the *E. coli* Nissle 1917 wild-type strain and the isogenic molybdenum-cofactor-deficient mutant in the presence of the indicated electron acceptors under anaerobic conditions. **c**, Competitive growth of *E. coli* NRG857c wild-type strain and the isogenic molybdenum-cofactor-deficient mutant in the presence of the indicated electron acceptors under anaerobic conditions. In **a**–**c**, $n = 3$ replicates per condition; n denotes the number of biological replicates. Data are shown as geometric mean and geometric s.d. of three experiments.

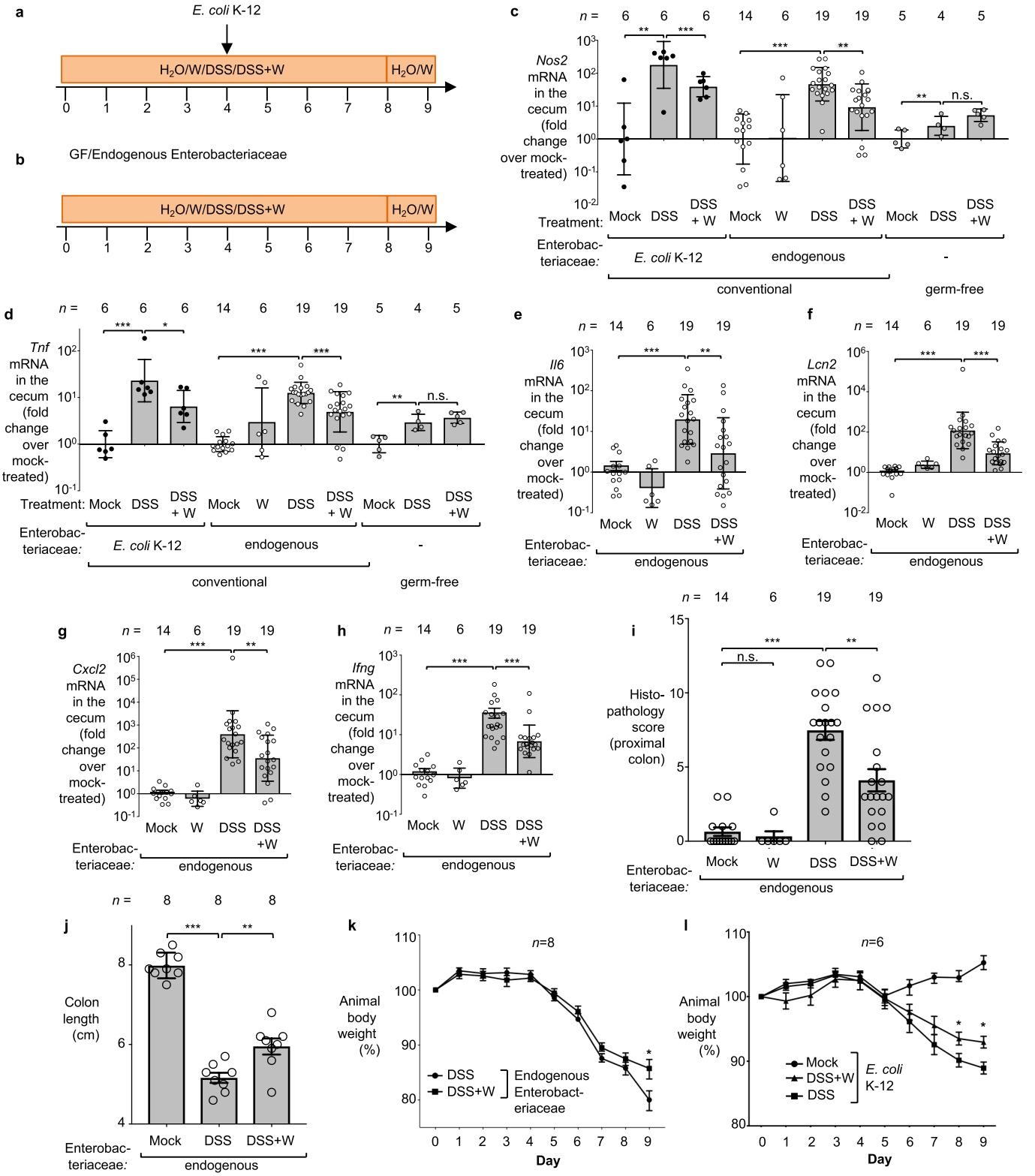

Extended Data Figure 2 | Tungstate treatment of mice colonized with *E. coli* K-12. Conventionally raised C57BL/6 mice were treated with 0.2% sodium tungstate, DSS, DSS plus sodium tungstate or left untreated (mock). After four days, animals were inoculated orally with the *E. coli* K-12 wild-type strain and the isogenic *moaA* mutant. C57BL/6 mice with naive microbiota (endogenous Enterobacteriaceae only) or germ-free C57BL/6 mice were treated similarly but were not inoculated with *E. coli* indicator strains. Samples were analysed after a total of nine days of treatment. **a**, **b**, Schematic representations of the colitis models. **c**–**h**, Transcription of *Nos2* (**c**), *Tnf* (**d**), *Il6* (**e**), *Lcn2* (**f**), *Cxcl2* (**g**) and *Ifng* (**h**) in the caecal mucosa was determined by RT–qPCR. *E. coli* K-12: $n = 6$ per group. Endogenous Enterobacteriaceae: mock, $n = 14$; W, $n = 6$; DSS, $n = 19$; DSS+W, $n = 19$. Germ-free: mock, $n = 5$; DSS, $n = 4$; DSS+W, $n = 5$. **i**, Cumulative histopathology score for the colon tissue; mock, $n = 14$; W, $n = 6$; DSS, $n = 19$; DSS+W, $n = 19$; data are shown as mean and s.e.m. and each dot represents one animal. **j**, Colon length, $n = 8$ per group. **k**, Body weight of mice harbouring endogenous Enterobacteriaceae, $n = 8$ per group. **l**, Body weight of mice experimentally colonized with *E. coli* K-12, $n = 6$ per group. Unless otherwise noted, data are shown as geometric mean and geometric s.d.

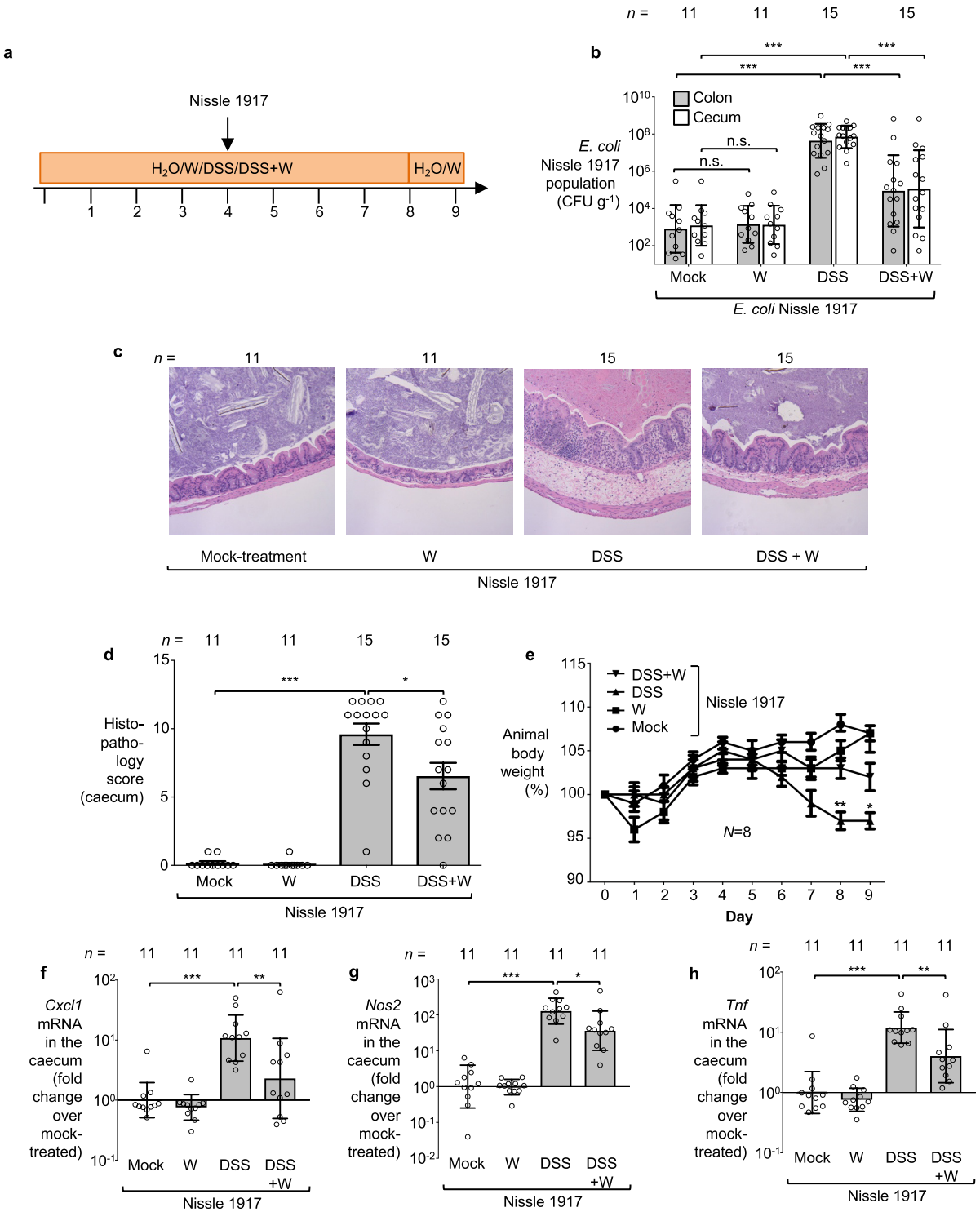

Extended Data Figure 3 | Effect of tungstate treatment on mice experimentally colonized with *E. coli* Nissle 1917. Groups of conventionally raised C57BL/6 mice were orally inoculated with the *E. coli* Nissle 1917 wild-type strain and treated with 0.2% sodium tungstate, DSS, DSS and sodium tungstate, or left untreated (mock) for nine days. **a**, Schematic representation of colitis model used in this figure. **b**, Bacterial load in the caecum (white bars) and colon content (grey bars). **c**, Formalin-fixed, haematoxylin and eosin-stained sections of the caecum were scored for the presence of inflammatory lesions; representative images of stained caecal sections. **d**, Cumulative histopathology score for the caecum tissue; data are shown as mean and s.e.m., and each dot represents one animal. In **b**–**d**, mock and tungsten, $n = 11$ per group; DSS and DSS+W, $n = 15$ per group. **e**, Animal body weight, $n = 8$ per group. **f**–**h**, Transcription of the inflammatory marker genes *Cxcl1* (**f**), *Nos2*, (**g**) and *Tnf* (**h**) in the caecal mucosa was determined by RT–qPCR, $n = 11$ per group. Unless otherwise noted, data are shown as geometric mean and geometric s.d.

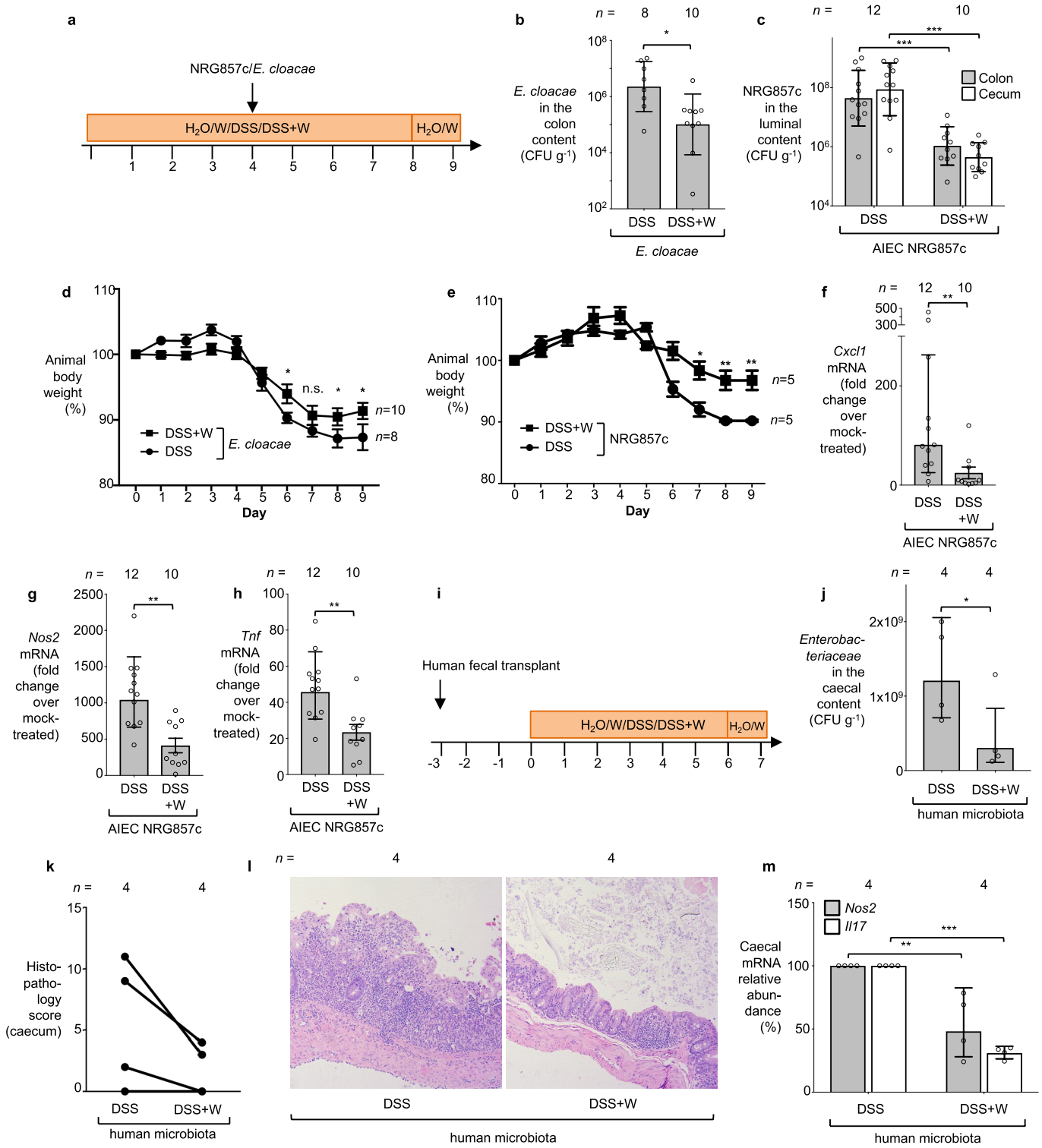

Extended Data Figure 4 | Effect of tungstate treatment on mice experimentally colonized with *Enterobacter cloacae* and adherent invasive *E. coli*. **a**–**h**, Conventionally raised C57BL/6 mice were treated with DSS or DSS plus tungstate. After four days, animals were inoculated intragastrically with the indicated bacterial strains. Samples were collected five days after inoculation. **a**, Schematic representation of the experiments. **b**, **c**, The total population of *E. cloacae* (**b**) and NRG857c (**c**; DSS, $n = 12$; DSS+W, $n = 10$) in the large intestinal content was determined by plating on selective medium. **d**, **e**, Animal body weight. In **b** and **d**: DSS, $n = 8$; DSS+W, $n = 10$. In **e**, $n = 5$ per group. **f**–**h**, Transcription levels of the inflammatory marker genes *Cxcl1* (**f**), *Nos2* (**g**) and *Tnf* (**h**) in the caecal mucosa were determined by RT–qPCR; DSS, $n = 12$; DSS+W, $n = 10$. **i**–**m**, Paired germ-free Swiss–Webster mice received human faecal transplants and were treated with DSS or DSS plus 0.2% sodium tungstate for seven days; DSS, $n = 4$; DSS+W, $n = 4$. **i**, Schematic representation of the experiments. **j**, The abundance of Enterobacteriaceae in the caecal content was determined by plating on selective medium (MacConkey agar). **k**, Formalin-fixed, haematoxylin and eosin-stained sections of the mouse caecum were scored for the presence of inflammatory lesions; **l**, representative images. **m**, Transcription levels of the inflammatory marker genes *Nos2* and *Il17* in the mouse caecal mucosa. Data are shown as geometric mean and geometric s.d.

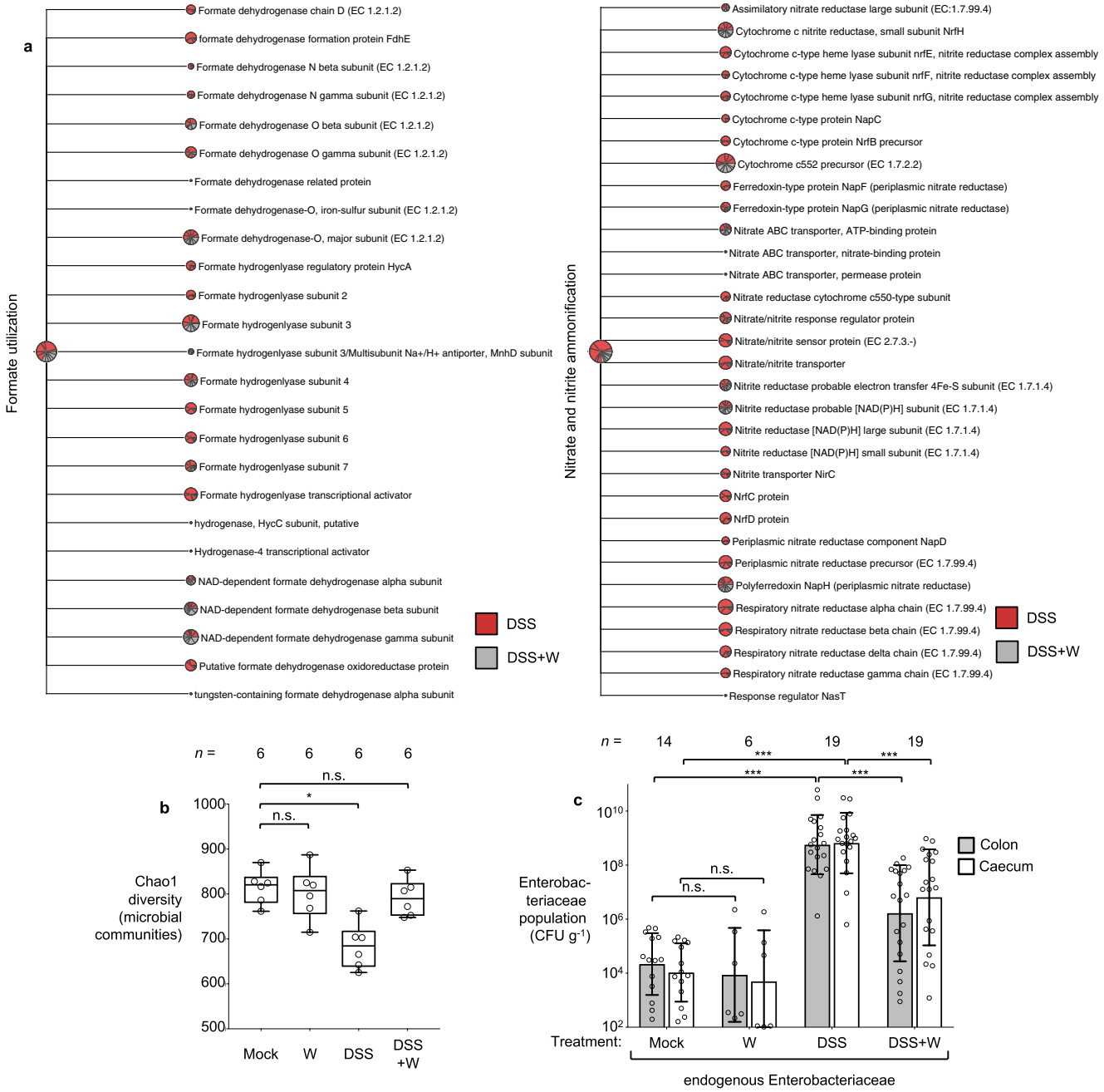

Extended Data Figure 5 | Effect of tungstate on the naive gut microbiome. Groups of C57BL/6 mice naturally harbouring Enterobacteriaceae were treated with 0.2% sodium tungstate, DSS, DSS plus tungstate or mock treatment for nine days (see also Extended Data Fig. 3b). **a**, Relative abundance of genes involved in formate and nitrate utilization in the caecal content shown by shotgun metagenomic sequencing (MEGAN5). Each section of the pie chart is representative of the number of mapped reads obtained for the individual animals ($n = 6$ per group). **b**, Box-and-whisker plot (boxes show median, first and third quantiles, whisker denotes minimum to maximum range) of Chao1 alpha diversity of the caecal microbiota community based on 16S profiling ($n = 6$ per group). **c**, Abundance of endogenous Enterobacteriaceae family members determined by plating on selective medium (MacConkey agar, **c**): mock, $n = 14$; W, $n = 6$; DSS, $n = 19$; DSS+W, $n = 19$. Data are shown as geometric mean and geometric s.d.

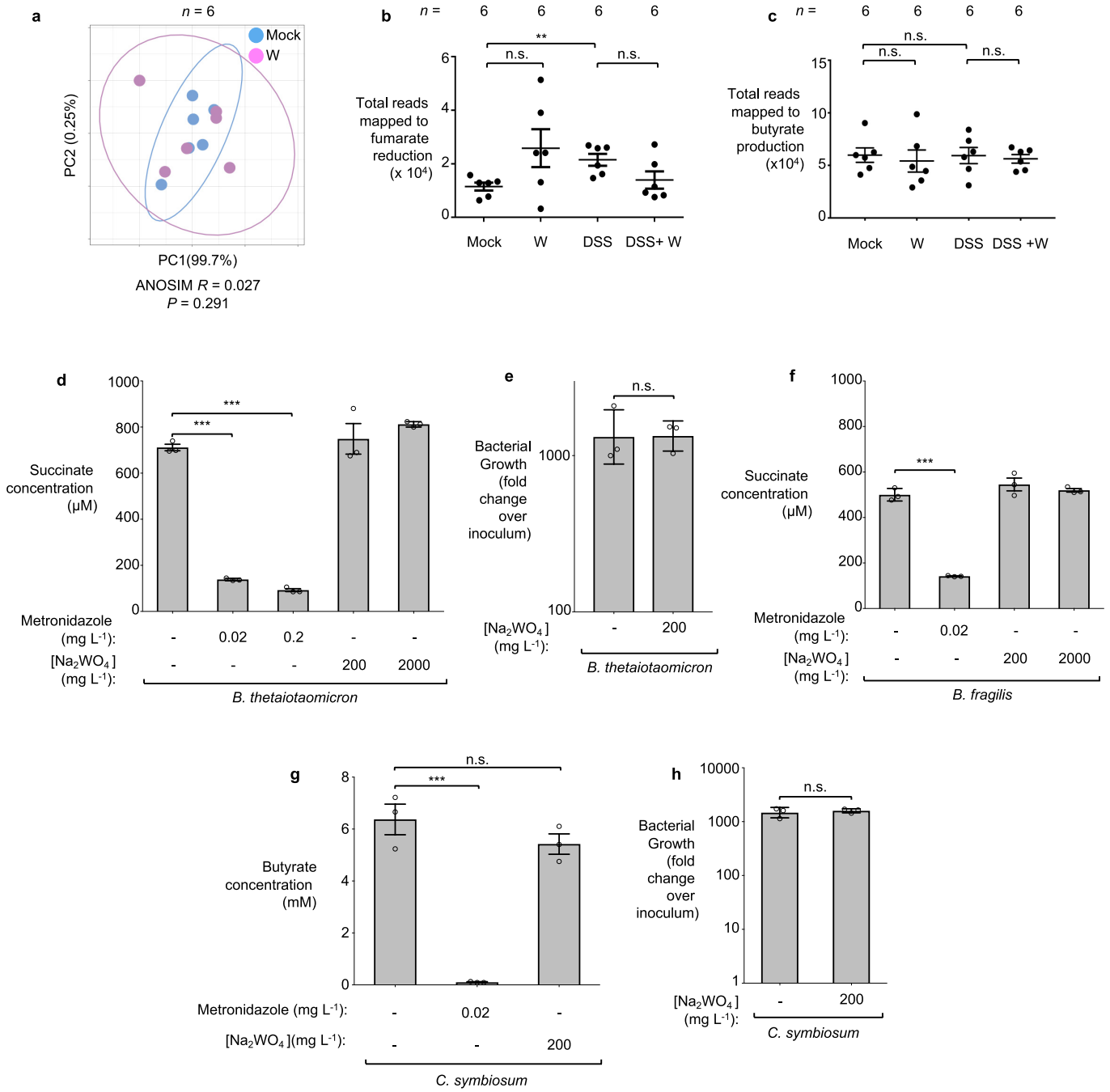

Extended Data Figure 6 | Effect of tungstate treatment on obligate anaerobic commensal bacteria. a–c, Metagenomic analysis of the caecal content of mice described in Extended Data Fig. 3b. Principal coordinates analysis of global metabolic pathway (**a**) and quantification of reads involved in fumarate respiration (**b**) and butyrate production (**c**). Ellipses in **a** denote 95% confidence interval. Data are shown as mean and s.d; $n = 6$ per group. **d–f**, *Bacteroides thetaiotaomicron* or *Bacteroides fragilis* were cultured anaerobically in mucin broth at 37 °C for 48 h. The medium was supplemented with sodium tungstate or metronidazole as indicated. Succinate production by *B. thetaiotaomicron* (**d**) and *B. fragilis* (**f**) was assessed by GC–MS. The growth of *B. thetaiotaomicron* was quantified by plating serial dilutions of bacterial culture on blood agar (**e**). **g**, *C. symbiosum* was inoculated into chopped meat broth and incubated anaerobically at 37 °C for 36 h. Butyrate concentration in the medium was measured using GC–MS. **h**, *C. symbiosum* was cultured anaerobically in chopped meat broth at 37 °C for 48 h. The growth of *C. symbiosum* was determined by plating serial dilutions of bacterial culture on thioglycolate plates. $n = 3$ biological replicates per condition. Data are shown as geometric mean and geometric s.d. of three experiments.

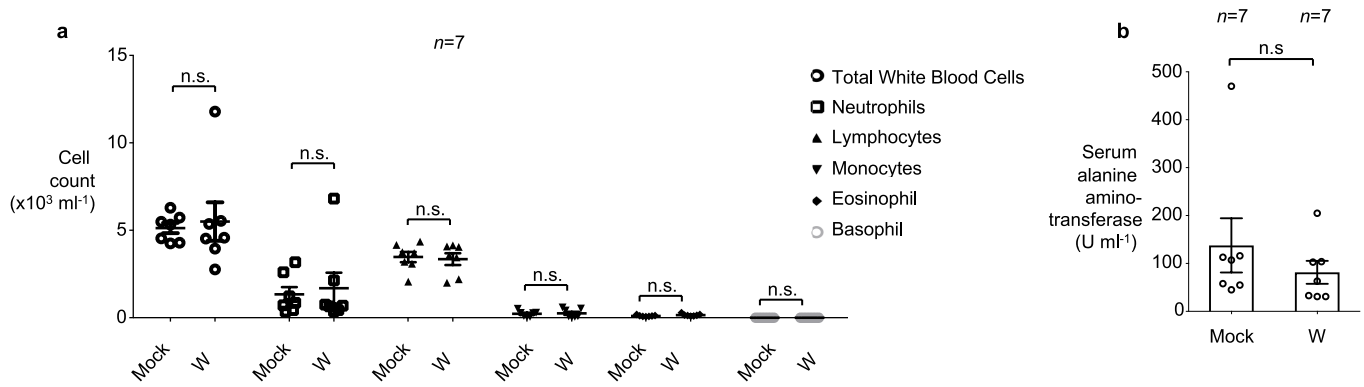

Extended Data Figure 7 | Assessment of overall health of mice treated orally with tungstate. Groups of seven mice were either mock-treated or treated with 0.2% sodium tungstate in drinking water for nine days. **a**, Complete blood count. **b**, Serum alanine amino-transferase concentration. $n = 7$ animals per group. Data are shown as geometric mean and geometric s.d.

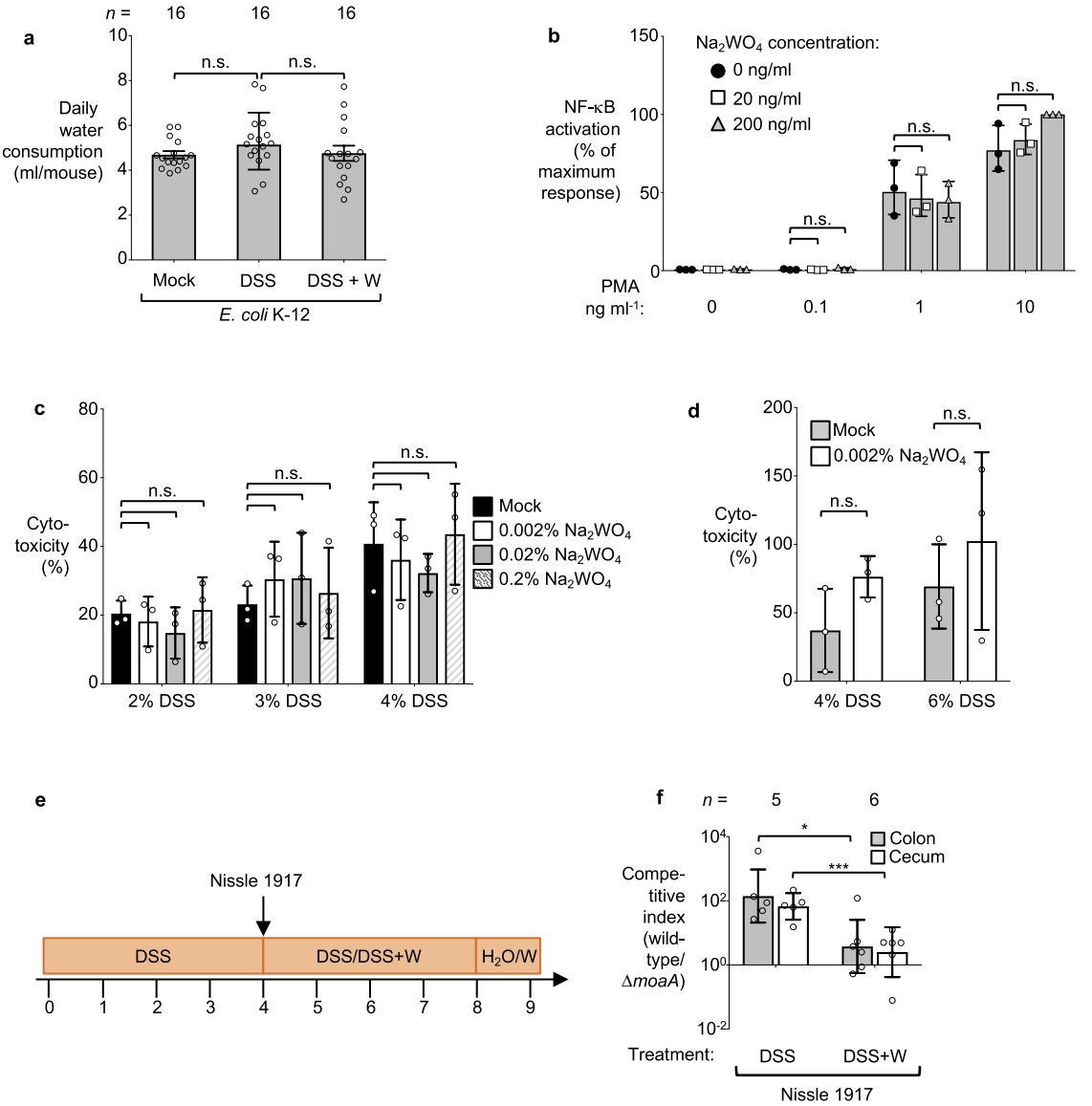

Extended Data Figure 8 | Exposure of cultured cells to sodium tungstate. a, Daily water consumption of mice inoculated with *E. coli* K-12. Each dot represents the average daily water consumption (ml per day) of three mice, obtained at eight time points, with two cages per treatment group, $n = 16$. **b**, HeLa57A cells, expressing luciferase under the control of a NF-κB-dependent promoter, were treated with PMA and sodium tungstate at the indicated concentrations. Relative luciferase activity was determined after 5 h. **c**, **d**, MODE-K or BMDMs cells were treated with DSS or DSS plus sodium tungstate at the indicated concentrations for 24 h. The release of lactate dehydrogenases into the culture supernatant by MODE-K cells (**c**) or BMDMs (**d**) was measured. In **b**–**d**, $n = 3$ biological replicates per condition. **e**, **f**, Groups of conventionally raised C57BL/6 mice were treated with DSS for four days. Animals were inoculated intragastrically with an equal mixture of the indicated *E. coli* Nissle 1917 wild-type strain and an isogenic *moaA* mutant. On the day of inoculation, a subset of mice was switched to DSS plus sodium tungstate for four days while a control group remained on DSS treatment. Schematic representation of experiment (**e**). The competitive index in the caecal (white bars) and colon content (grey bars) was analysed 5 days after inoculation (**f**; DSS, $n = 5$; DSS+W, $n = 6$). Data are shown as geometric mean and geometric s.d.

nature research

Corresponding author(s): Dr. Sebastian Winter

☐ Initial submission ☐ Revised version ☒ Final submission

Life Sciences Reporting Summary

Nature Research wishes to improve the reproducibility of the work that we publish. This form is intended for publication with all accepted life science papers and provides structure for consistency and transparency in reporting. Every life science submission will use this form; some list items might not apply to an individual manuscript, but all fields must be completed for clarity.

For further information on the points included in this form, see Reporting Life Sciences Research. For further information on Nature Research policies, including our data availability policy, see Authors & Referees and the Editorial Policy Checklist.

Experimental design

1. Sample size

Describe how sample size was determined.

All studies are pilot / exploratory studies. It is impossible to predict the magnitude of the variation between animals as well as the effect size for a particular parameter based on our current knowledge. The group sizes determined for each experimental design (at least 5 animals per treatment group) represent the minimal number of animals needed to achieve a significant difference of p .05 between experimental groups for the non-parametric Mann–Whitney–Wilcoxon U test (in case data are not normally distributed).

2. Data exclusions

Describe any data exclusions.

Mice that were euthanized early due to health concerns were excluded from the analysis

3. Replication

Describe whether the experimental findings were reliably reproduced.

All attempts to replicate the experiments were successful.

4. Randomization

Describe how samples/organisms/participants were allocated into experimental groups.

Animals were randomly assigned to groups (cages) prior to any experimentation (line 411-414, 442-445,462-464).

5. Blinding

Describe whether the investigators were blinded to group allocation during data collection and/or analysis.

Histopathology analysis was performed in a blinded manner. (line 538-543).

Note: all studies involving animals and/or human research participants must disclose whether blinding and randomization were used.

6. Statistical parameters

For all figures and tables that use statistical methods, confirm that the following items are present in relevant figure legends (or in the Methods section if additional space is needed).

n/a	Confirmed
☐	☒ The exact sample size (*n*) for each experimental group/condition, given as a discrete number and unit of measurement (animals, litters, cultures, etc.)
☐	☒ A description of how samples were collected, noting whether measurements were taken from distinct samples or whether the same sample was measured repeatedly
☐	☒ A statement indicating how many times each experiment was replicated
☐	☒ The statistical test(s) used and whether they are one- or two-sided (note: only common tests should be described solely by name; more complex techniques should be described in the Methods section)
☒	☐ A description of any assumptions or corrections, such as an adjustment for multiple comparisons
☐	☒ The test results (e.g. *P* values) given as exact values whenever possible and with confidence intervals noted
☐	☒ A clear description of statistics including central tendency (e.g. median, mean) and variation (e.g. standard deviation, interquartile range)
☐	☒ Clearly defined error bars

See the web collection on statistics for biologists for further resources and guidance.

Software

Policy information about availability of computer code

7. Software

Describe the software used to analyze the data in this study.

16S sequencing data was subjected to a standard workflow for processing and quality assessment of the raw 16S sequence data and the downstream phylogenetic analysis. The pipeline consists of an initial customized Linux-based command script for trimming, demultiplexing, and quality filtering the raw PE sequence data generated by Illumina system. Sequence alignment, operational taxonomic units (OTUs) picking against the Greengenes reference collection, clustering, phylogenetic and taxonomic profiling, permanova analysis, and the analysis of beta diversity (principle component analysis) on the demultiplexed sequences were performed with the Quantitative Insights into Microbial Ecology QIIME open source software package 26.
Sample collection, shotgun metagenomics sequencing and data analysis were performed as previously described (Ref. 11).
In this study, reads mapped to the SEED database were exported from MEGAN5 into BIOM tables, which were subjected to Analysis of similarity (ANOSIM) in Qiime (Ref.26) and Principle Component Analysis (PCA) using STAMP (Ref. 27). To map reads to bacterial metabolic genes, a total of 100 each of the butyrate production operons (bcdAB, but and ato) and succinate dehydrogenase operon (sdhABC) were downloaded from the KEGG database. Sequences were clustered to remove redundancy using cdhit-est (Ref. 28,29) with a sequence identity threshold of 0.9. Paired end reads were mapped to these gene clusters using the BBmap tool with the following settings: qtrim=lr, minid=0.90, ambig=random, covstats=true.

For manuscripts utilizing custom algorithms or software that are central to the paper but not yet described in the published literature, software must be made available to editors and reviewers upon request. We strongly encourage code deposition in a community repository (e.g. GitHub). *Nature Methods* guidance for providing algorithms and software for publication provides further information on this topic.

Materials and reagents

Policy information about availability of materials

8. Materials availability

Indicate whether there are restrictions on availability of unique materials or if these materials are only available for distribution by a for-profit company.

There is no restriction to material availability.

9. Antibodies

Describe the antibodies used and how they were validated for use in the system under study (i.e. assay and species).

No antibodies were used in the study.

10. Eukaryotic cell lines

a. State the source of each eukaryotic cell line used.

HeLa57A: Rodriguez MS, Thompson J, Hay RT, Dargemont C. 1999. Nuclear retention of IkappaBalpha protects it from signal-induced degradation and inhibits nuclear factor kappaB transcriptional activation. J. Biol. Chem. 274:9108 –9115. (R. T. Hay, the Wellcome Trust Centre for Gene Regulation and Expression, College of Life Sciences, University of Dundee, United Kingdom).
MODE-K: Vidal K, Grosjean I, evillard JP, Gespach C, Kaiserlian D. 1993. Immortalization of mouse intestinal epithelial cells by the SV40-large T gene. Phenotypic and immune characterization of the MODE-K cell line. J Immunol Methods. 1993 Nov 5;166(1):63-73. (D. Kaiserlian, Unité d'Immunologie et de Stratégie Vaccinale, Institut Pasteur de Lyon, France).

b. Describe the method of cell line authentication used.

The cell lines were not authenticated.

c. Report whether the cell lines were tested for mycoplasma contamination.

Cell lines were not tested for mycoplasma contamination.

d. If any of the cell lines used are listed in the database of commonly misidentified cell lines maintained by ICLAC, provide a scientific rationale for their use.

None of the cell lines used are listed in the ICLAC database.

Animals and human research participants

Policy information about studies involving animals; when reporting animal research, follow the ARRIVE guidelines

11. Description of research animals

Provide details on animals and/or animal-derived materials used in the study.

DSS colitis model and sodium tungstate treatment. All experiments involving mice were approved by the Institutional Animal Care and Use Committee at UT Southwestern Medical Center (APN#T-2013-0159) and UC Davis (APN#16196). Female 9-12 week old C57BL/6J wild-type mice were obtained from the Jackson Laboratory (Bar Harbor) or Charles River Laboratory (Morrisville), as indicated. Mice were randomly assigned into cages before the experiment. The drinking water was replaced with either filter-sterilized water (mock-treatment), or a filter-sterilized solution of 0.2% (w/v) sodium tungstate (Sigma, St Louis), or a filter-sterilized solution of 2% or 3% (w/v) dextran sulfate sodium (DSS; relative molecular mass 36,000 – 50,000; MP Biomedicals) in water at the indicated concentrations, or a filter-sterilized solution of DSS and 0.2% (w/v) sodium tungstate. In one experiment, tungsten was administered in a sodium tungstate-fortified diet (1000 ppm). At the indicated time points, animals were orally inoculated with either 0.1 ml of LB broth or 0.1 ml LB broth containing 1 x 10^9 CFU E. coli, or remained uninfected. In the competitive colonization experiments, animals were inoculated with 5 x 10^8 CFU of each E. coli or E. cloacae strain. One day prior to the end of the experiment, the drinking water was switched for 24 h to regular, filter-sterilized water to reduce the amount of DSS present in the samples. After euthanization, colonic and cecal tissue were collected, flash frozen and stored at -80°C for subsequent mRNA and protein expression analysis. Fecal material, cecal content, and colonic content were harvested in sterile PBS and the bacterial load for the E. coli strains or Enterobacteriaceae was numerated by plating serial 10-fold dilutions on LB plates supplemented with appropriate antibiotic or MacConkey Agar plates, respectively. Germ-free C57BL/6 mice were maintained in plastic gnotobiotic isolators on a 12-hour light cycle. DSS-mediated colitis was induced in 8-12 week old germ-free mice, following the protocol described above.
Piroxicam-accelerated colitis model in conventional Il10-/- mice. Conventional Il10-/- mice on C57BL/6 (males only) backgrounds were randomly assigned into cages before orally inoculated with 1 x 10^9 CFU of mouse AIEC NC101. Regular mouse chow was replaced with Piroxicam-fortified diet (100 ppm; Teklad custom research diets, Envigo) and changed daily. Drinking water was either replaced with filter-sterilized water (mock) or a filter-sterilized solution of 0.2% (w/v) sodium tungstate. After 14 days, mice were euthanized and the samples were collected as described above.
Germ-free Swiss Webster mice were maintained in plastic gnotobiotic isolators on a 12-hour light cycle. Mice were randomized, paired and orally gavaged with endoscopy samples from the patients listed in the table at the end of this section. The colonization was allowed to proceed for 3 days before mice receiving DSS or DSS plus sodium tungstate for 7 days. Mice were euthanized and the samples were collected as described above.

Policy information about studies involving human research participants

12. Description of human research participants

Describe the covariate-relevant population characteristics of the human research participants.

All procedures involving human subjects were reviewed and approved by the institutional review board at the University of Texas Southwestern Medical Center (IRB#112010-130). Written informed consent was obtained from all participants or parents/legal guardians of participating minors. Except for the study PI and study coordinator, all study personnel handling these samples did not have access to personal identification information. Patients were considered for fecal donation if they had an established diagnosis of inflammatory bowel disease, had active disease at the time of collection and were free from antibiotic use over the past 3 months. Patient characteristics from samples used are summarized in Supplementary Table 4. Human fecal samples were obtained at time of colonoscopy by direct endoscopic aspiration of fecal contents from patients with active colonic disease. A total of 10ml of liquid fecal material was collected from each patient and aliquoted into 1ml cryovials. The samples were then snap frozen in liquid nitrogen and stored at -80°C until used.